

# Alkylammonium-Based Protic Ionic Liquids Part I: Preparation and Physicochemical Characterization

Mérièm Anouti,\* Magaly Caillon-Caravanier, Corinne Le Floch, and Daniel Lemordant

Université François Rabelais, Laboratoire CIME (EA2098), Parc de Grandmont, 37200 Tours, France

Received: April 22, 2008; Revised Manuscript Received: May 16, 2008

Novel alkylammonium-cation-based protic acid ionic liquids (PILs) were prepared through a simple and atom-economic neutralization reaction between an amine, such as diisopropylmethylamine, and diisopropylethylamine, and a Brønsted acid, HX, where X is  $\text{HCOO}^-$ ,  $\text{CH}_3\text{COO}^-$ , or  $\text{HF}_2^-$ . The density, viscosity, acidic scale, electrochemical window, temperature dependency of ionic conductivity, and thermal properties of these PILs were measured and investigated in detail. Results show that protonated alkylammonium such as *N*-ethyl-diisopropyl formate and *N*-methyl-diisopropyl formate are liquid at room temperature and possess very low viscosities, that is, 18 and 24 cP, respectively, at 25 °C. An investigation of their thermal properties shows that they present a wide liquid range up to  $-100$  °C and a heat thermal stability up to 350 °C. Alkylammonium-based PILs have a relatively low cost and low toxicity and show a high ionic conductivity (up to  $8 \text{ mS cm}^{-1}$ ) at room temperature. They have wide applicable perspectives for fuel cell devices, thermal transfer fluids, and acid-catalyzed reaction media and catalysts as replacements of conventional inorganic acids.

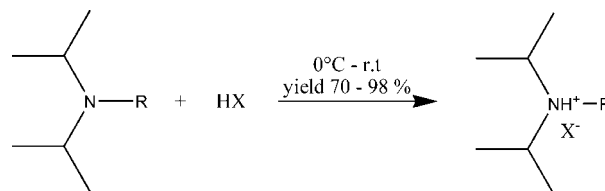
## 1. Introduction

Ionic liquids (ILs) usually refer to organic salts having a melting points below 100 °C and composed exclusively of ions. They are increasingly employed<sup>1,2</sup> and should progressively replace usual solvents in many chemical processes as green organic solvents.<sup>3–7</sup> This is mainly because they possess several specific physicochemical properties such as nonvolatility, nonflammability,<sup>2,3,8</sup> and excellent thermal and chemical stability and have a stable liquid range of more than 400 °C. Moreover, some ILs present a wide electrochemical windows and a high ionic conductivity. Thanks to their high polarity, ILs are expected to be very suitable solvents for reactions between organic soluble and water soluble reagents.

Room-temperature ILs (RTILs) are ILs which are liquid at room temperature or at slightly high temperature (20–30 °C). Those formed by the transfer of protons from Brønsted acids to Brønsted bases form a protic subgroup in the class of ambient temperature fluid system now referred as protic ILs (PILs). Proton-conducting electrolyte are now emerging as useful material because of their various possibilities of application such as electrolyte in aqueous batteries, fuel cells, double-layer capacitors, dye-sensitized solar cell, or actuators.<sup>9–19</sup> These promise large new fields of application for PILs.

RTILs are usually based on quaternary ammonium  $[\text{R}_4\text{N}]^+$  or aromatic and saturated cyclic amine salts. Likewise, anions may be based on both inorganic and organic groups. Lately, *N*-protonated 1-alkylimidazolium salts were prepared by several research groups: as an example, He et al.<sup>20</sup> used successfully *N*-protonated 1-methylimidazolium tetrafluoroborate as a Brønsted acid catalyst in esterification and carbonyl protection. ILs prepared from protonated imidazole and bis(trifluoromethanesulfonyl)amide could be used as a proton-conducting nonaqueous electrolyte in fuel cell devices. However, the main disadvantages of imidazolium-based ILs are their relatively high cost

## SCHEME 1: Preparation of ILs



and toxicity in general chemical applications. Therefore, the development of lower cost and lower intrinsic toxicity room temperature ILs is highly desired.

We report in the present work the preparation of new tertiary ammonium-based PILs containing  $\text{HF}_2^-$ ,  $\text{CH}_3\text{COO}^-$ , and  $\text{HCOO}^-$  anions obtained by neutralization of diisopropylethylamine or diisopropylmethylamine by a Brønsted acid. Physicochemical properties of these PILs are determined and discussed according to the modification of the cation and the anion.

## 2. Experimental Section

**2.1. Materials.** All amines and organic acids used in this study are commercially available from Fluka (>99,0%) and used without further purification. The hydrofluoric acid solution (50% in water) is obtained from Sigma Aldrich. Water is purified with a Milli-Q 18,3 MΩ water system, and 1,2-dichloroethane DCE (>99,0%) is purchased from Sigma Aldrich.

**2.2. Preparation of RTILs.** The preparation of alkyl ammonium-based ILs is illustrated by the following equation (Scheme 1).

The nature of the R substituent and the  $\text{X}^-$  anion are both reported in Table 1a with the abbreviation of the obtained PILs.

**Preparation of Diisopropylalkylammonium Formate and Acetate PILs.** The example of DIPEF (1a) shows a typical preparation method, and a similar procedure is used with compounds 1b, 2a, and 2b. *N*-ethyl-*N*-isopropylpropan-2-amine

\* Corresponding author. E-mail: meriem.anouti@univ-tours.fr. Fax: (33)247367360. Tel: (33)247366951.

TABLE 1A: Names and Abbreviations of the PILs

X <sup>-</sup>	name	abbreviation
R = CH <sub>3</sub> CH <sub>2</sub> <sup>-</sup>		
HCOO <sup>-</sup>	diisopropylethylammonium formate	DIPEF (1a)
CH <sub>3</sub> COO <sup>-</sup>	diisopropylethylammonium acetate	DIPEAc (1b)
HF <sub>2</sub> <sup>-</sup>	diisopropylethylammonium hydrogenbisfluoride	DIPEHF (1c)
R = CH <sub>3</sub> <sup>-</sup>		
HCOO <sup>-</sup>	diisopropylmethylammonium formate	DIPMF (2a)
CH <sub>3</sub> COO <sup>-</sup>	diisopropylmethylammonium acetate	DIPMAc (2b)
HF <sub>2</sub> <sup>-</sup>	diisopropylmethylammonium hydrogenbisfluoride	DIPMHF (2c)

(25.8 g, 0.2 mol) is placed in a three-neck round-bottom flask immersed in an ice bath and equipped with a reflux condenser, a dropping funnel to add the acid, and a thermometer to monitor the temperature. Under vigorous stirring, formic acid (7.5 mL, 0.2 mol) is added dropwise to the amine (60 min). Because this acid–base reaction is strongly exothermic, the mixture temperature is maintained under 25 °C during the addition of the acid by use the ice bath. Then, stirring continues for 4 h at ambient temperature until a less viscous liquid decantate. This new phase can be clear (1a, 2a) or yellow-colored (1b, 2b). The residual amine and/or acid is evaporated under reduced pressure, and the remaining liquid is further dried at 80 °C under reduced pressure (1–5 mmHg). Neither crystallization nor solidification was observed on the liquid, which was stored for several weeks at 20 °C.

**Preparation of Diisopropylalkylammonium Hydrogenbisfluoride PILs.** *N*-ethyl-*N*-isopropylpropan-2-amine (25.8 g, 0.2 mol) and *N*-methyl-*N*-isopropylpropan-2-amine (23.0 g, 0.2 mol) are introduced in a two-necked round-bottom flask immersed in an ice bath and equipped with a plastic dropping funnel to add the hydrofluoric acid 50% in water and a thermometer to control the temperature. Under vigorous stirring, hydrofluoric acid (16 mL, 0.4 mol) is added dropwise to the flask in about 60 min (mixture temperature <35 °C). Stirring is maintained for 2 h at ambient temperature before adding 120 mL of DCE. Then, this mixture is distilled under normal pressure until a heteroazeotrope boiling point is obtained to get rid of the residual water thanks to the water–DCE azeotrope. DCE is finally evaporated from the mixture under reduced pressure so that a clear and viscous liquid can be collected.

<sup>1</sup>H NMR spectrum are obtained by using a Bruker 200 MHz spectrometer, CDCl<sub>3</sub> as solvent, and TMS as internal standard.

**2.3. Measurements.** Densities are determined by the weight method at 25 °C. Measurements of refractive index are realized at 25 °C with a ABBE refractive index instrument, calibrated with deionized water. Viscosities are measured by using a TA instrument rheometer (AR 1000) with conical geometry at various temperatures (from 25 to 80 °C). Ionic conductivities are measured by using a Crison (GLP 31) digital conductimeter at several frequencies. The temperature control (from 20 to 200 °C) is ensured by a JULABO thermostatted bath. PILs' electrochemical windows are checked by linear voltammetry at ambient temperature by using an EGG M 270A Electrochemical Work Station and a three-electrode configuration. A 3 mm diameter carbon is used as a working electrode, a platinum wire as a counter electrode, and an Ag/AgCl<sub>sat</sub>, KCl<sub>sat</sub>(PIL) electrode as a reference. The reference system is determinate exactly versus SHE electrode with a ferrocenium ion/ferrocene system:  $E_{\text{ref}} = 0.216 \text{ mV/SHE}$ .

The measurement of the PILs Brønsted acidity scale is conducted on a Perkin-Elmer Lambda 25 UV visible spectrophotometer with a methyl red indicator.

Differential scanning calorimetry (DSC) is carried out on a Perkin-Elmer DSC6 under a N<sub>2</sub> atmosphere. Samples for DSC measurements are sealed in Al pans. Thermograms are recorded during cooling (from 10 to –120 °C) at a scan rate of 5 °C·min<sup>-1</sup> and heating (from 10 to 400 °C) with a scan rate of 10 °C·min<sup>-1</sup>. Differential thermal analyzer (ATG) is measured on a Perkin-Elmer thermogravimetry instrument with a scan rate of 10 °C·min<sup>-1</sup> under N<sub>2</sub> atmosphere in Pt pans.

### 3. Results and Characterizations

**3.1. <sup>1</sup>H NMR.** <sup>1</sup>H NMR spectrums (200 MHz, CDCl<sub>3</sub>, TMS) of these ILs show that the protons resonate in the  $\delta$  ranges summarized in Table 1b.

When D<sub>2</sub>O is added, the signal due to the hydrogen carried by the nitrogen is the only one to disappear.

**3.2. Physical Properties of PILs. Refractive index.** The refractive index is related to the polarizability/dipolarity of the environment. Data relative to studied PILs are shown in Table 1b. These results are quite comparable to values for typical organic solvents and similar to the values reported for the alkylammonium IL salts studied by Shetty et al.<sup>21</sup>

**Density.** Density of ILs is typically in the range 1.2–1.6 g·cm<sup>-3</sup>.<sup>22</sup> However, some ILs (for example, those based on the dicyanoamide anion, [N(CN)<sub>2</sub>]<sup>-</sup>)<sup>23</sup> show a density lower than 1 g·cm<sup>-3</sup>. In general, the densities of ILs decrease with increasing length of the alkyl chain in the cation. For example, in ILs composed of substituted imidazolium cations and CF<sub>3</sub>SO<sub>3</sub><sup>-</sup> anions, the density decreases from 1.39 g·cm<sup>-3</sup> for [EMIm]<sup>+</sup> to 1.33 g·cm<sup>-3</sup> for [EEIm]<sup>+</sup> and from 1.29 g·cm<sup>-3</sup> for [BMIm]<sup>+</sup> to 1.27 g·cm<sup>-3</sup> for [BEIm]<sup>+</sup>. The densities of ILs are also affected by the identity of anions. For example, the densities of 1-butyl-3-methylimidazolium-type ILs with different anions, such as BF<sub>4</sub><sup>-</sup>, PF<sub>6</sub><sup>-</sup>, TFA<sup>-</sup>, and Tf<sub>2</sub>N<sup>-</sup> are equal to 1.12 g·cm<sup>-3</sup>, 1.21 g·cm<sup>-3</sup>, 1.36 g·cm<sup>-3</sup>, and 1.43 g·cm<sup>-3</sup>, respectively.<sup>24</sup> In our study, the salts have significantly low densities (0.982–1.055 g·cm<sup>-3</sup>), comparable to that of water.

**Viscosity.** Generally, ILs are more viscous than common molecular solvents ( $\eta(\text{H}_2\text{O}) = 0.89 \text{ cP}$  at 25 °C). Indeed, their viscosities typically range from 30 cP to about 100 cP at room temperature, but in some cases, values as high as 500–600 cP are observed. The viscosity of synthesized PILs measured at 25 °C are low, 18 cP (1a) and 25 cP (2a) for DIPEF and DIPMF, respectively, but the association of the same cations with acetate ion leads to slightly more viscous salts, 35 cP for (1b) and 55 cP for (2b). The ability of anions to form hydrogen bonds has a significant effect on viscosity. Fluorinated anions such as HF<sub>2</sub><sup>-</sup> give viscous ILs (80 cP for (1c) and 100 cP for (3c)) because of the formation of hydrogen bonding. Still, these values remain very low compared to those of ILs based on alkyl imidazolium cation. For example, the viscosities of some usual air and water stable ILs at room temperature are 312 cP for [BMIm]PF<sub>6</sub>,<sup>25</sup> 180 cP for [BMIm]BF<sub>4</sub>,<sup>26</sup> 52 cP for [BMIm]TF<sub>2</sub>N,<sup>24</sup> and 85 cP for [BMPy]TF<sub>2</sub>N,<sup>27</sup> as shown in the literature. As the temperature increases, all ILs show a significant decrease in viscosity. The dependence of conductivity and viscosity on the temperature and the addition of water will be discussed in later in this article.

**Conductivity.** ILs have reasonably good ionic conductivities compared to those of organic solvents/electrolyte systems (up to 10 mS cm<sup>-1</sup>).<sup>22</sup> However, at room temperature, their conductivities are usually lower than those of concentrated aqueous electrolytes, on the basis that ILs are composed exclusively by ions. The conductivity at 25 °C of the six PILs under study falls between 1.3 and 8.2 mS·cm<sup>-1</sup> (Table 2). These values are comparable to those of the most conductive ILs

TABLE 1B:  $^1\text{H}$  NMR Spectrum Characteristics of the PILs

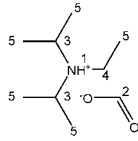
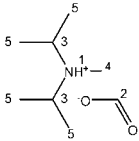
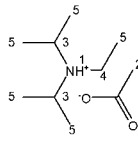
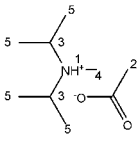
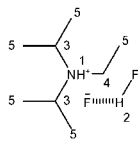
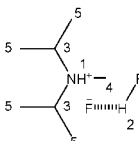
PILs	$\delta$ in ppm	PILs	$\delta$ in ppm
 DIPEF (1a)	1 9.6, s, 1H	 DIPMF (2a)	1 5.6, s, 1H
	2 8.4, s, 1H		2 8.4, s, 1H
	3 3.5, broad signal, 2H		3 3.4, broad signal, 2H
	4 3.1, q, 2H		4 2.5, s, 3H
	5 1.5, broad signal, 15H		5 1.5, broad signal, 12H
 DIPEAc (1b)	1 10.5, s, 1H	 DIPMAc (2b)	1 11.3, s, 1H
	2 2.0, s, 3H		2 2.1, s, 3H
	3 3.5, broad signal, 2H		3 3.4, broad signal, 2H
	4 3.1, q, 2H		4 2.5, s, 3H
	5 1.3, broad signal, 15H		5 1.3, broad signal, 12H
 DIPEHF (1c)	1 8.2, s, 1H	 DIPMHF (2c)	1 7.7, s, 1H
	2 10.2, s, 1H		2 10.3, s, 1H
	3 3.6, broad signal, 2H		3 3.6, broad signal, 2H
	4 3.1, q, 2H		4 2.6, s, 3H
	5 1.4, d, 15H		5 1.4, d, 12H

TABLE 2: Refractive Index, Specific Gravity, Molar Volume, Viscosity, and Specific and Equivalent Ionic Conductivity of PILs at 25 °C

ILs	$n_D \pm 0.05\%$	$\rho \text{ (g}\cdot\text{cm}^{-3}) \pm 0.1\%$	$V_m \text{ (cm}^3\cdot\text{mol}^{-1}) \pm 0.1\%$	$\eta \text{ (cP)} \pm 0.1\%$	$\sigma \text{ (mS}\cdot\text{cm}^{-1}) \pm 2\%$	$\Lambda \text{ (S}\cdot\text{cm}^2\cdot\text{mol}^{-1}) \pm 2\%$
DIPEF (1a)	1.4480	1.015	172.68	18.0	5.0	0.86
DIPEAc (1b)	1.4435	0.982	201.93	54.4	1.3	0.26
DIPMF (2a)	1.4465	1.002	160.82	25.0	8.2	1.32
DIPMAc (2b)	1.4380	0.995	176.04	32.2	1.6	0.28
DIPEHF (1c)	1.4205	1.003	168.75	81.1	3.4	0.57
DIPMHF (2c)	1.4095	1.055	148.08	100.0	7.6	1.12

TABLE 3: Electrochemical Windows (V) of PILs at 25 °C

PILs	electrochemical windows <sup>a</sup> (V) at 25 °C
DIPEF (1a)	2.7
DIPEAc (1b)	2.6
DIPMF (2a)	2.7
DIPMAc (2b)	2.6
DIPEHF (1c)	2.3
DIPMHF (2c)	2.2

<sup>a</sup> Defined as the potential redox with a current of  $\pm 1 \text{ mA}\cdot\text{cm}^{-2}$ .

among salts based on tetraalkylammonium ( $[\text{Me}_2\text{EtPrN}]^+$   $[\text{N}(\text{CF}_3\text{SO}_2)_2]^-$ ,  $\sigma = 1.2 \text{ mS}\cdot\text{cm}^{-1}$ ;  $[\text{nOctBu}_3\text{N}]^+[\text{N}(\text{CF}_3\text{SO}_2)_2]^-$ ,  $\sigma = 0.13 \text{ mS}\cdot\text{cm}^{-1}$ ;  $[\text{MePrPp}]^+[\text{N}(\text{CF}_3\text{SO}_2)_2]^-$ ,  $\sigma = 1.51 \text{ mS}\cdot\text{cm}^{-1}$  <sup>29</sup>), pyrrolidinium ( $[\text{nPrMePy}]^+[\text{N}(\text{CF}_3\text{SO}_2)_2]^-$ ,  $\sigma = 1.4 \text{ mS}\cdot\text{cm}^{-1}$ ;  $[\text{nBuMePy}]^+[\text{N}(\text{CF}_3\text{SO}_2)_2]^-$ ,  $\sigma = 2.2 \text{ mS}\cdot\text{cm}^{-1}$  <sup>27</sup>), pyridinium ( $[\text{BuPi}]^+[\text{N}(\text{CF}_3\text{SO}_2)_2]^-$ ,  $\sigma = 2.2 \text{ mS}\cdot\text{cm}^{-1}$  <sup>30</sup>), and imidazolium ( $[\text{EtMeIm}]^+[\text{CF}_3\text{SO}_3]^-$ ,  $\sigma = 8.6 \text{ mS}\cdot\text{cm}^{-1}$ ;  $[\text{EtMeIm}]^+[\text{CH}_3\text{CO}_2]^-$ ,  $\sigma = 2.8 \text{ mS}\cdot\text{cm}^{-1}$  <sup>24</sup>), the conductivity range of which is situated between 0.1 and  $10 \text{ mS}\cdot\text{cm}^{-1}$ . Both ILs based on acetate anion present the lowest conductivity,  $\sigma = 1.3 \text{ mS}\cdot\text{cm}^{-1}$  for DIPEAc and  $\sigma = 1.6 \text{ mS}\cdot\text{cm}^{-1}$  for DIPMAc, but the largest conductivity is interpreted by anion. PILs which possess the formate anion  $\text{HCOO}^-$  present the highest conductivity,  $\sigma = 5.0 \text{ mS}\cdot\text{cm}^{-1}$  for DIPEF and  $\sigma = 8.2 \text{ mS}\cdot\text{cm}^{-1}$  for DIPMF. The conductivity of ILs is inversely proportional to their viscosity, according to the Stokes law, but ion aggregation by H-bonding as in hydrogenbisfluoride solution has also to be taken into account

and could affect drastically the conductivity ( $\sigma = 7.6 \text{ mS}\cdot\text{cm}^{-1}$  for DIPMHF). Therefore, conductivities of PILs are difficult to predict.

**Electrochemical Stability.** Electrolytes for electrochemical devices should resist to reduction and oxidation and exhibit a convenient electrochemical window. The electrochemical window of PILs was measured at room temperature by using a vitreous-carbon working electrode and Ag/AgCl-in-ILs reference electrode. The results obtained show stability window ranges

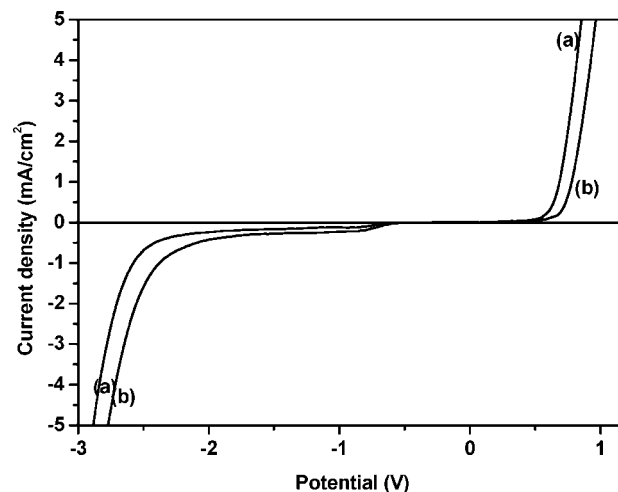
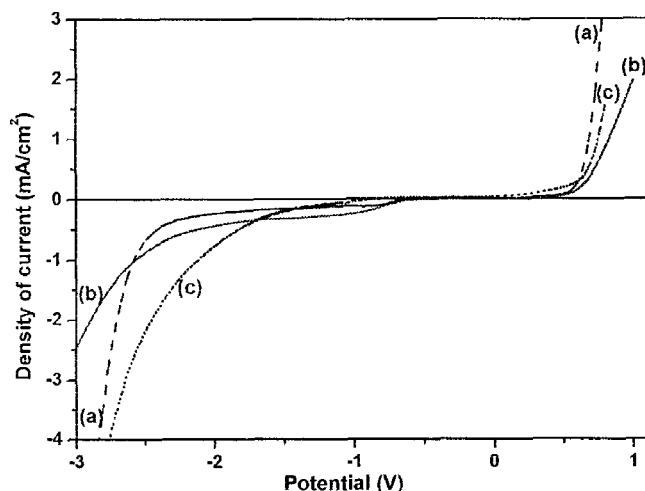
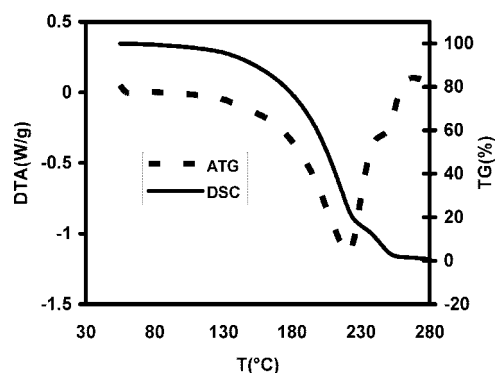


Figure 1. Linear voltammogram recorded at vitreous carbon electrode versus the Ag/AgCl<sub>sat</sub>, KCl<sub>sat</sub>(IL) reference electrode of DIPEF (a) and DIPMF (b) at a scan rate of  $100 \text{ mV}\cdot\text{s}^{-1}$ .



**Figure 2.** Linear voltammogram recorded at vitreous carbon electrode versus the  $\text{Ag}/\text{AgCl}_{\text{sat.}}/\text{KCl}_{\text{sat.}}(\text{IL})$  reference electrode of DIPEF (a), DIPEAc (b), and DIPEHF (c) at a scan rate of  $100 \text{ mV} \cdot \text{s}^{-1}$ .



**Figure 3.** ATG and DSC thermogram for DIPEHF at  $5 \text{ K} \cdot \text{min}^{-1}$  in the temperature range  $30\text{--}280 \text{ }^{\circ}\text{C}$ .

from 2.2 to 2.7 V (Table 3). A typical linear voltammogram of DIPEF, DIPMF, DIPEAc, and DIPEBF is shown in Figures 1 and 2. The electrochemical window of studied PILs is less than that obtained for aprotic salts such as  $[\text{nBuMePy}]^+ [\text{N}(\text{CF}_3\text{SO}_2)_2]^-$ , 5.5 V<sup>31</sup> and  $[\text{nMePrPp}]^+ [\text{N}(\text{CF}_3\text{SO}_2)_2]^-$ , 5.6 V.<sup>32</sup> The carboxylate anion is oxidized at a relatively low anodic potential, +0.7 V versus  $\text{Ag}/\text{AgCl}$  reference, whereas the alkylammonium cation shows a cathodic reduction at a very negative potential,  $-2.5 \text{ V}$  versus  $\text{Ag}/\text{AgCl}$  reference. We observe on Figures 1 and 2 a little wave of reduction of low intensity toward  $-0.7 \text{ V}$  because of the free  $\text{H}^+$  ions resulting from the dissociation of the formic acid residual (Figure 1, curves a and b and figure 2, curve a) or acetic acid (Figure 2, b)). In the case of the hydrofluoric acid strongly associated, the  $\text{H}^+$  ions are not reducible as shown by curve c in Figure 2. Stability windows obtained at Pt and vitreous-carbon working electrodes are comparable.

The nature of substituents on the ammonium cation does not modify electrochemical windows, as can be noticed on the graph reported in Figure 1, but the cation reduction potential depends on the counterion. Indeed,  $\text{HF}_2^-$  anion (curve c, Figure 2)

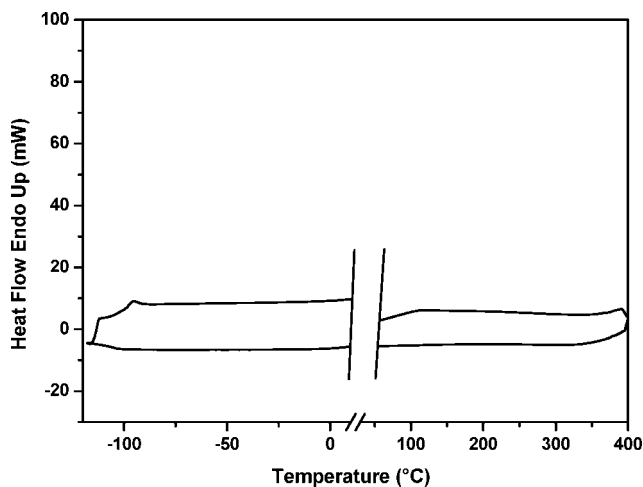


**Figure 4.** DSC thermograms of DIPMF in the low-temperature range (from  $20$  to  $-120 \text{ }^{\circ}\text{C}$ ) at  $5 \text{ K} \cdot \text{min}^{-1}$  scan rate and in the high-temperature range (from  $20$  to  $400 \text{ }^{\circ}\text{C}$ ) at  $10 \text{ K} \cdot \text{min}^{-1}$  scan rate.

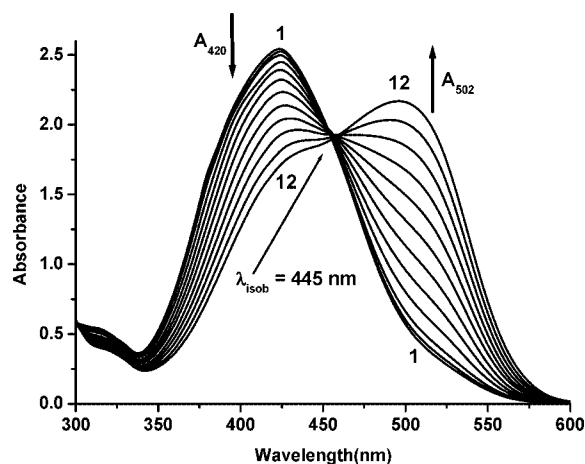


**Figure 5.** Absorption spectra of methyl red for various concentrations of  $\text{HCOOH}$  in DIPEF.

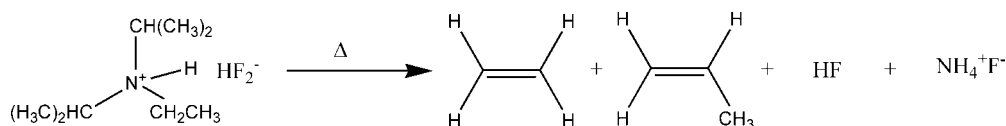
**TABLE 4: Thermal Stability of PILs**

PILs	DIPEF	DIPMF	DIPEAc	DIPMAc	DIPEHF	DIPMHF
$T_d$ (K)	>653	>653	>653	>653	363	363
$T_g$ (K)	170	167	179	172	218	198

reduces the stability window from 0.7 V compared to the acetate ion (curve b, Figure 2).

**Thermal properties.** ILs can be thermally stable up to  $450 \text{ }^{\circ}\text{C}$ . The thermal stability of ILs is defined by the strength of their heteroatom-carbon and heteroatom-hydrogen bonds. Wilkes et al. reported<sup>33</sup> that the ILs 1-ethyl-3-methyl-imidazolium tetrafluoroborate, 1-butyl-3-methyl-imidazolium tetrafluoroborate, and 1,2-dimethyl-3-propyl imidazolium bis(trifluoromethylsulfonyl)imide are stable up to 445, 423, and  $457 \text{ }^{\circ}\text{C}$ , respectively. Our experiments show that the synthesized ILs do not present any melting or crystallization temperature. They remain in a liquid state down to a very low temperature where they vitrify ( $T_g$ ). This behavior, rarely observed for ILs, is attributed to the

## SCHEME 2: Degradation Reaction of DIPEHF





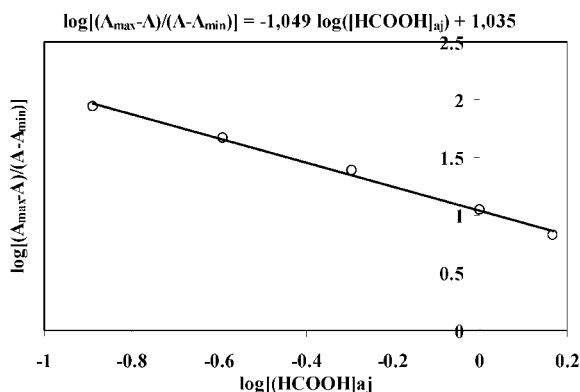


**Figure 6.** Variation of Hammett's functions  $H_0$  for various concentrations of formic acid in DIPEF.

**TABLE 5: Calculation of the Hammett's Function of HCOOH in DIPEF**

$[H^+]$ mol·L <sup>-1</sup>	$A_{502}$	$(A_{\max} - A)/(A - A_{\min})$	$\log([I^-]/[HI])$	$H_0 (\pm 0.05)$
0.129	0.5336	86.87	1.9388	6.93
0.257	0.5657	46.40	1.6665	6.66
0.509	0.6262	24.38	1.3869	6.38
0.999	0.7681	11.14	1.0469	6.04
1.470	0.9280	6.65	0.8227	5.82
1.924	1.1044	4.43	0.6464	5.64

small size of the anions and the dissymmetry resulting from isopropyl and ethyl or methyl substituents on the ammonium cation. Moreover, it can be noticed that among the ILs, only the  $HF_2^-$  anion decomposed after 89 °C, as can be seen on the ATG reported in Figure 3.

This early decomposition is due to a degradation reaction of the ammonium cation induced by the transformation of  $HF_2^-$  ions into HF and  $F^-$  at high temperature as described in Scheme 2.

Indeed, when compounds (1c) and (2c) are heated over 100 °C, a white-colored precipitate of ammonium fluoride  $NH_4F$  can be observed.

For the four other compounds (1a), (1b), (2a), and (2b), neither decomposition ( $T_d$ ) nor boiling ( $T_{eb}$ ) temperatures are observed up to 390 °C, as can be seen on the thermogram reported Figure 4. Compared to anions, the nature of cations has a lower impact on the thermal stability of the Alkyl-based ILs. All  $T_g$  and  $T_d$  of the PILs are shown in Table 4.

**3.3. Acidity-Scale Determination.** Determining a Brønsted acidity scale for ILs aims at finding an interrelation between their catalytic activities and their acidities for various acid–base reactions. Protons' acidity is mainly defined by their solvation. Indeed, faintly solvated protons show a higher chemical activity. Protons' properties in those environments depend on ILs nature and the strength of the acid providing the anion in its composition. In a recent study, Thomazeau et al.<sup>34</sup> have reported an observation on the behavior of various Brønsted acids soluble in ILs. The Brønsted acidity has been estimated from the determination of Hammett's acidity functions  $H_0$  by using UV–visible spectroscopy.

Various volumes of HCOOH containing methyl red dye indicator, with  $pK(I)_{aq} = 5$ , are added to DIPEF (S solvent). As Figure 5 shows (curves 1–12), a decrease can be observed in the absorption band due to the basic form  $I^-$  at  $\lambda = 420$  nm which is progressively replaced with that of the protonated form HI at  $\lambda = 502$  nm. The bundle of curves passes by an isobestic point at about  $\lambda = 445$  nm, indicating the protonation equilibrium of the dye indicator,  $I^- + H^+ \rightleftharpoons HI$ .

The absorption at 502 nm is all along due to the two indicator forms,  $A = \varepsilon_{HI}l[HI] + \varepsilon_{I^-}l[I^-]$ . By using  $C_1$  for the whole initial concentration,  $C_1 = [I^-] + [HI]$ ,  $A_{\min}$  for the initial absorption at 420 nm only due to the basic form (curve 1 figure 5),  $A_{\min} = \varepsilon_{I^-}lC_1$ ,  $A_{\max}$  for the final absorption at 502 nm of the totally protonated indicator in the presence of an acid excess,  $A_{\max} = \varepsilon_{HI}lC_1$ , it can be written as  $[I^-]_s/[HI]_s = (A_{\max} - A)/(A - A_{\min})$ . The  $K_{HI}$  protonation equilibrium constant for the indicator is  $K(HI)_s = [H^+]_s[I^-]_s/[HI]_s$ , and it can then be written as

$$pK(HI)_s = H_0 - \log\left(\frac{A_{\max} - A}{A - A_{\min}}\right) \quad (1)$$

where  $H_0$  is the Hammett's function

$$H_0 = -\log a(H^+_{aq}) - \log\left(\frac{\gamma(I^-)}{\gamma(HI)}\right) + \log\left(\frac{\Gamma(I^-)}{\Gamma(HI)}\right) \quad (2)$$

with  $\gamma(I^-)$  and  $\gamma(HI)$  representing the activity coefficients for the nonprotonated and the protonated form of the indicator, respectively, and  $\Gamma(I^-)$  and  $\Gamma(HI)$  representing their activity coefficients to the transfer from the aqueous phase in the S solvent. At infinite dilution,  $H_0$  is identified by  $H_0 = -\log [H^+]$ , and eq 1 can then be written as

$$\log\left(\frac{A_{\max} - A}{A - A_{\min}}\right) = -pK(HI)_s + pKa(HCOOH)_s - \log\left(\frac{[HCOOH]_{aq}}{[HCOO^-]}\right) \quad (3)$$

where  $[HCOO^-]$  is the molarity of the IL, nearly constant during the acid addition.

When plotting  $\log(A_{\max} - A)/(A - A_{\min})$  versus  $-\log [HCOO^-]$ , a line with a slope of 1 is obtained (Figure 6). The y-intercept  $b$  corresponds to  $b = -pK(HI)_s + pKa(HCOOH)_s + \log [HCOO^-]$ . If the equilibrium constant of the dye indicator  $pK(HI)_s$  in the PIL is supposed to have the same value as in an aqueous environment, we have  $pK(HI)_s = pK(HI)_{aq} = 5.0$ . We then get  $pKa(HCOOH)_s = 5.4$ ; therefore, the formic acid seems weaker in a PILs DIPEF environment than in an aqueous environment where  $pKa(HCOOH)_{aq} = 3.2$ . Moreover, observing the Hammett's constants  $H_0$  for  $[H^+] = 130$  mmol·L<sup>-1</sup> shows that the DIPEF is a neutral environment compared with  $[BMIM][HNTf_2]$  ( $H_0 = -4.70$ ).<sup>34</sup>

As the acid concentration increases, the absorptions of the HI indicator protonated form, monitored at 340 nm, decreases. The indicator nonprotonated form (when no acid is added to IL, see Figure 5, curve 1) enables to define the ratio  $[I^-]/[HI]$  from the absorptions measured at each acid addition (curves 2–5, Figure 5); Hammett's function is then calculated (Table 5, DIPEF).

## 4. Conclusion

The six alkyl-based Brønsted acid PILs examined here were prepared by a simple atom-economic neutralization reaction. The density, viscosity, acidity scale, electrochemical window, conductivity, and phase behavior were measured and investigated in detail. The resulting physical properties show that the effect of anion identity is preponderant. As a result, simple variations in cation and anion structure or overall, ionic composition illustrate the ease with which physical properties of a class of PILs can be modified to produce a wide range of solvents. These PILs could be produced easily in large amounts and have potentially wide applicable perspectives for fuel cell electrolytes, thermal transfer fluids, and acid-catalyzed reaction

environments or catalysts as replacements for conventional inorganic acids.

## References and Notes

- (1) Wilkes, J. S. *Green Chem.* **2002**, 4, 73.
- (2) Welton, T. *Chem. Rev.* **1999**, 99, 2071.
- (3) Dupont, J.; deSouza, R. F.; Suarez, P. A. *Chem. Rev.* **2002**, 102, 3667.
- (4) Earle, M. J.; Seddon, K. R. *Pure Appl. Chem.* **2000**, 72, 1391.
- (5) Wasserscheid, P.; Keim, W. *Angew. Chem.* **2000**, 112, 3926.
- (6) Holbrey, J. D.; Seddon, K. R. *Clean Prod. Proc.* **1999**, 1, 223.
- (7) Heintz, A. J. *J. Chem. Thermodyn.* **2005**, 37, 525.
- (8) Ngo, H. L.; LeCompte, K.; Hargens, L.; McEwen, A. B. *Thermochem. Acta* **2000**, 357, 97.
- (9) Ogihara, W.; Sun, J.; Forsyth, M.; MacFarlane, D. R.; Yoshizawa, M.; Ohno, H. *Electrochim. Acta* **2004**, 49, 1797.
- (10) Nakagawa, H.; Izuchi, S.; Kuwana, K.; Nukuda, T.; Aihara, Y. *J. Electrochem. Soc.* **2003**, 150, 695.
- (11) Doyle, M.; K Choi, S.; Proulx, G. J. *Electrochem. Soc.* **2000**, 147, 34.
- (12) Susan, M. A. H.; Noda, A.; Mitsushima, S.; Watanabe, M. *Chem. Commun.* **2003**, 938.
- (13) Lewandowski, A.; Swiderska, A. *Solid State Ionics* **2003**, 161, 243.
- (14) Ue, M.; Takeda, M.; Toriumi, A.; Kominato, A.; Hagiwara, R.; Ito, Y. *J. Electrochem. Soc.* **2003**, 150, 499.
- (15) Lewandowski, A.; Galinski, M. *J. Phys. Chem. Solids* **2004**, 65, 281.
- (16) Matsumoto, H.; Matsuda, T.; Tsuda, T.; Hagiwara, R.; Ito, Y.; Miyazaki, Y. *Chem. Lett.* **2001**, 30, 26.
- (17) Mikoshiba, S.; Murai, S.; Sumino, H.; Hayase, S. *Chem. Lett.* **2002**, 31, 1156.
- (18) Wang, P.; Zakeeruddin, S. M.; Comte, P.; Exnar, I.; Gratzel, M. *J. Am. Chem. Soc.* **2003**, 125, 1166.
- (19) Lu, W.; Fadeev, A. G.; Qi, B.; Smela, E.; Mattes, B. R.; Ding, J.; Spinks, G. M.; Mazurkiewics, J.; Zhou, D.; Wallace, G. G.; MacFarlane, D. R.; Forsyth, S. A.; Forsyth, M. *Science* **2002**, 297, 983.
- (20) Zhu, H. P.; Yang, F.; Tang, J.; He, M. Y. *Green Chem.* **2003**, 5, 38.
- (21) Shetty, P. H.; Youngberg, P. J.; Kersten, B. R.; Poole, C. F. *J. Chromatogr.* **1987**, 411, 61.
- (22) Galinski, M. *Electrochim. Acta* **2006**, 51, 5567.
- (23) MacFarlane, D. R.; Golding, J.; Forsyth, S.; Forsyth, M.; Deacon, G. B. *Chem. Commun.* **2001**, 1430.
- (24) Bonhote, P.; Dias, A. P.; Papageorgiou, N.; Kalyanasundaram, K.; Gratzel, M. *Inorg. Chem.* **1996**, 35, 1168.
- (25) Carda-Broch, S.; Berthod, A.; Armstrong, A. W. *Anal. Bioanal. Chem.* **2003**, 375, 191.
- (26) Nishida, T.; Tashiro, Y.; Yamamoto, M. *J. Fluorine Chem.* **2003**, 120, 135.
- (27) MacFarlane, D. R.; Sun, J.; Golding, J.; Meakin, P.; Forsyth, M. *Electrochim. Acta* **2000**, 45, 1271.
- (28) Sun, J.; Foreyth, M.; MacFarlane, D. R. *J. Phys. Chem. B* **1998**, 102, 8858.
- (29) Owens, G. S.; Abu-Omar, M. M. *J. Mol. Catal. A: Chem.* **2002**, 187, 215.
- (30) Fuller, J.; Carlin, R. T.; DeLong, H. C.; Haworth, D. *J. Chem. Soc. Chem. Commun.* **1994**, 299.
- (31) MacFarlane, D. R.; Meakin, P.; Sun, J.; Amini, N.; Forsyth, M. *J. Phys. Chem. B* **1999**, 103, 4164.
- (32) Noda, A.; Watanabe, M. *Electrochim. Acta* **2000**, 45, 1265.
- (33) Wilkes, J. S. *J. Mol. Catal. A: Chem.* **2004**, 214, 11.
- (34) Thomazeau, C.; Olivier-Bourbigou, H.; Magna, L.; Luts, S.; Gilbert, B. *J. Am. Chem. Soc.* **2003**, 125, 5264.

JP803483F